



P2-type Na_{2/3}Ni_{1/3}Mn_{2/3-x}Ti_xO₂ as a new positive electrode for higher energy Na-ion batteries

Journal:	<i>ChemComm</i>
Manuscript ID:	CC-COM-12-2013-049856.R1
Article Type:	Communication
Date Submitted by the Author:	27-Jan-2014
Complete List of Authors:	Yoshida, Hiroaki; Tokyo University of Science, ; Tokyo University of Science, Department of Applied Chemistry Yabuuchi, Naoaki; Tokyo University of Science, Department of Applied Chemistry Kubota, Kei; Tokyo University of Science, Department of Applied Chemistry Ikeuchi, Issei; Tokyo University of Science, Department of Applied Chemistry Garsuch, Arnd; BASF SE, Schulz-Dobrick, Martin; BASF SE, Komaba, Shinichi; Tokyo University of Science, Department of Applied Chemistry

COMMUNICATION

Cite this: DOI: 10.1039/x0xx00000x

Received 00th January 2012,

Accepted 00th January 2012

DOI: 10.1039/x0xx00000x

www.rsc.org/

P2-type $\text{Na}_{2/3}\text{Ni}_{1/3}\text{Mn}_{2/3-x}\text{Ti}_x\text{O}_2$ as a new positive electrode for higher energy Na-ion batteries

Hiroaki Yoshida,^a Naoaki Yabuuchi,^a Kei Kubota,^a Issei Ikeuchi,^a Arnd Garsuch,^b Martin Schulz-Dobrick,^b and Shinichi Komaba^{a*}

New electrode materials of layered oxides, $\text{Na}_{2/3}\text{Ni}_{1/3}\text{Mn}_{2/3-x}\text{Ti}_x\text{O}_2$ ($0 \leq x \leq 2/3$), are successfully synthesized, and their electrochemical performance is examined in aprotic Na cells. A Na// $\text{Na}_{2/3}\text{Ni}_{1/3}\text{Mn}_{1/2}\text{Ti}_{1/6}\text{O}_2$ cell delivers 127 mAh g^{-1} of reversible capacity and average voltage reaches 3.7 V at first discharge with good capacity retention.

Recently, the research interest for Na-ion batteries is rapidly increasing, and materials researchers have been exploring new sodium insertion materials for the battery applications¹. Our group has reported iron-based materials as promising positive electrode²⁻⁴. Among sodium insertion materials, layered Na_xMeO_2 (Me = metallic element) compounds have been intensively studied as electrode materials, especially for battery applications⁵⁻¹⁰. Layered Na_xMeO_2 compounds can be categorized into two main groups using the classification proposed by Delmas et al.¹¹; O3 type or P2 type, in which the sodium ions are accommodated at octahedral and prismatic site sandwiched between MeO_2 slabs, respectively. In particular, P2-type $\text{Na}_{2/3}\text{Fe}_{1/2}\text{Mn}_{1/2}\text{O}_2$ and O3-type $\text{NaFe}_{0.5}\text{Co}_{0.5}\text{O}_2$ can deliver 200 and 160 mAh g^{-1} of reversible capacity, respectively, with relatively good capacity retention^{2, 4}. However, average operating voltage of Na_xMeO_2 (vs. Na^+/Na) is generally lower (~ 1.0 V) than that of Li_xMeO_2 (vs. Li^+/Li). Since energy density is calculated by multiplying the discharge capacity by the average operating voltage, increase in the operating voltage is also of primary importance to realize high energy Na-ion batteries.

In this study, we focus on P2- $\text{Na}_{2/3}\text{Ni}_{1/3}\text{Mn}_{2/3-x}\text{Ti}_x\text{O}_2$, which shows relatively high operating voltage based on a $\text{Ni}^{2+}/\text{Ni}^{4+}$ redox reaction¹². However, discharge capacity of Na// $\text{Na}_{2/3}\text{Ni}_{1/3}\text{Mn}_{2/3}\text{O}_2$ cell fades rapidly during cycles by charging to 4.5 V; therefore, available reversible capacity is limited to only 80 mAh g^{-1} in lower potential domain than 3.8 V¹³. In this article, we report synthesis and electrode performance of titanium substituted $\text{Na}_{2/3}\text{Ni}_{1/3}\text{Mn}_{2/3-x}\text{Ti}_x\text{O}_2$ as novel positive electrode materials for Na-ion batteries. It is found that $\text{Na}_{2/3}\text{Ni}_{1/3}\text{Mn}_{1/2}\text{Ti}_{1/6}\text{O}_2$ delivers 127 mAh g^{-1} of reversible capacity with 3.7 volts of average discharge voltage with superior cycle life. As a result, estimated energy density of the hard carbon// $\text{Na}_{2/3}\text{Ni}_{1/3}\text{Mn}_{1/2}\text{Ti}_{1/6}\text{O}_2$ cell is calculated to be over 300 Wh kg^{-1} , corresponding to approximately 80% of energy density for a graphite//LiCoO₂ system.

^a Department of Applied Chemistry, Tokyo University of Science, 1-3 Kagurazaka, Shinjuku, Tokyo 162-8601, Japan. E-mail: komaba@rs.kagu.tus.ac.jp

^b BASF SE, GCN/EE - M311, 67056 Ludwigshafen, Germany

Electronic supplementary information (ESI) available: cycle retention tests with different cutoff voltage (Figures S1 and S2), and comparison of physical properties of samples is shown in Table. S1. See DOI.

$\text{Na}_{2/3}\text{Ni}_{1/3}\text{Mn}_{2/3-x}\text{Ti}_x\text{O}_2$ ($x = 0, 1/6, 1/3, 2/3$) samples were prepared by a solid-state reaction. Stoichiometric mixture of reagent grade Na_2CO_3 , NiO, TiO_2 , and Mn_2O_3 was ball-milled in wet condition with acetone addition for 12 h at 600 rpm. The mixtures were dried and thus obtained powder was pressed into pellets. For the $\text{Na}_{2/3}\text{Ni}_{1/3}\text{Mn}_{2/3}\text{O}_2$ sample, the pellet was heated at 900 °C for 24 h in air according to the previous report¹². For the $\text{Na}_{2/3}\text{Ni}_{1/3}\text{Mn}_{2/3-x}\text{Ti}_x\text{O}_2$ ($x = 1/6, 1/3$) samples, the pellets were heated at 900 °C for 12 h in air. For the $\text{Na}_{2/3}\text{Ni}_{1/3}\text{Ti}_{2/3}\text{O}_2$ sample, the pellet was heated at 950 °C for 12 h in air. After the calcination, the samples were taken out from the heated furnace, and then immediately transferred into an argon-filled glove box. The samples cooled to room temperature in the glove box and were kept inside to avoid the contact with moisture in air. Crystal structures of the obtained samples were examined by using an X-ray diffractometer (MultiFlex, Rigaku Co., Ltd.) equipped with a high-speed position sensitive detector (D/teX Ultra, Rigaku Co., Ltd.). Non-monochromatized Cu K α radiation is utilized as an X-ray source with a nickel filter. The samples were covered with a laboratory made attachment during the data collection to avoid air exposure. For electrochemical test, coin-type cells (R2032 type) with $\text{Na}_{2/3}\text{Ni}_{1/3}\text{Mn}_{2/3-x}\text{Ti}_x\text{O}_2$ as positive electrodes were assembled in the argon filled glove box (dew point: < -70 °C). Positive electrodes consisted of 80 wt% prepared materials, 10 wt% acetylene black, and 10 wt% poly(vinylidene fluoride), which were mixed with *N*-methylpyrrolidone (Kanto Chemical Co., Ltd., Japan) and pasted onto Al foil, and then dried at 80 °C in vacuum. Metallic sodium foil is used as a negative electrode. Electrolyte solution used was 1.0 mol dm^{-3} NaPF₆ dissolved in propylene carbonate (battery grade, Kishida Chemical Co., Japan). A glass fibre filter (GB-100R, ADVANTEC Co.) was used as a separator.

Figure 1a compares X-ray diffraction (XRD) patterns of synthesized $\text{Na}_{2/3}\text{Ni}_{1/3}\text{Mn}_{2/3-x}\text{Ti}_x\text{O}_2$ ($x = 0, 1/6, 1/3, 2/3$) samples. Almost all the diffraction lines can be assigned into the P2-type layered structure with a trace amount of impurity (NiO for $x = 1/3$). A schematic illustration of the P2-type crystal structure is also shown in Fig. 1b. Lattice parameters, *a*- and *c*-axis values, are also plotted as a function of *x* in $\text{Na}_{2/3}\text{Ni}_{1/3}\text{Mn}_{2/3-x}\text{Ti}_x\text{O}_2$ in Fig. 1c. Lattice parameters linearly increase by the substitution of Ti for Mn, and its increase obeys Vegard's law with consideration of larger ionic size of Ti^{4+} than Mn^{4+} , suggesting that a solid solution is formed in the range of $0 \leq x \leq 2/3$ in $\text{Na}_{2/3}\text{Ni}_{1/3}\text{Mn}_{2/3-x}\text{Ti}_x\text{O}_2$.

Initial charge/discharge curves of Na cells (corresponding to sodium deintercalation/intercalation from/into $\text{Na}_{2/3-y}\text{Ni}_{1/3}\text{Mn}_{2/3-x}\text{Ti}_y\text{O}_2$, respectively) are compared in Fig. 2. Charge/discharge cut-off voltages are set to 4.5/2.5 V, except for Na// $\text{Na}_{2/3}\text{Ni}_{1/3}\text{Ti}_{2/3}\text{O}_2$ cell (4.2/2.5 V) to suppress large irreversible capacity above 4.2 V (see supporting information, Fig. S1). Reversible capacity of the

electrode is significantly influenced by the partial substitution of titanium. Ti-free $\text{Na}_{2/3}\text{Ni}_{1/3}\text{Mn}_{2/3}\text{O}_2$ ($x = 0$) delivers the highest discharge capacity among the solid solution samples. However, discharge capacity rapidly fades during cycles and only 67% of initial discharge capacity is retained after 10 cycles (in supporting information, Fig. S2). This fact is in good agreement with the recent report by Lee et al., and the insufficient capacity retention could originate from the P2/O2 phase transition by Na extraction with large volume change ($\sim 23\%$)¹³. In contrast, titanium-substituted samples demonstrate improved capacity retention even though initial reversible capacity decreases with the titanium substitution. The $\text{Na}/\text{Na}_{2/3}\text{Ni}_{1/3}\text{Mn}_{1/2}\text{Ti}_{1/6}\text{O}_2$ cell delivers 127 mAh g^{-1} of reversible capacity with ca. 3.7 V of average discharge voltage for initial cycle. Estimated energy density reaches 470 Wh kg^{-1} based on Na metal and approximately 94% of the reversible capacity is retained after 10 cycles. Moreover, the stepwise voltage profiles for $\text{Na}_{2/3}\text{Ni}_{1/3}\text{Mn}_{2/3}\text{O}_2$ obviously change by the titanium substitution, suggesting the suppression of Na/vacancy ordering, electronic/magnetic ordering and/or phase transition during sodium intercalation^{12, 13}. Ex-situ XRD study (not shown here) reveals that volume shrinkage of the fully charged state is effectively reduced from 23.1 % for Ti-free to 12-13% for Ti-substituted ones. SEM images of $\text{Na}_{2/3}\text{Ni}_{1/3}\text{Mn}_{2/3-x}\text{Ti}_x\text{O}_2$ electrodes are also shown in Fig. 2. Although the primary particle size of titanium substituted samples is not uniform, particle size of $\text{Na}_{2/3}\text{Ni}_{1/3}\text{Mn}_{1/2}\text{Ti}_{1/6}\text{O}_2$ ($\sim 5 \mu\text{m}$) with hexagonal plate-like morphology is larger than that of $\text{Na}_{2/3}\text{Ni}_{1/3}\text{Mn}_{2/3}\text{O}_2$ ($\sim 2 \mu\text{m}$).

Capacity retention of $\text{Na}/\text{Na}_{2/3}\text{Ni}_{1/3}\text{Mn}_{2/3-x}\text{Ti}_x\text{O}_2$ cells is further compared in Fig. 3a. Ti-doped samples show superior cyclability compared to the $\text{Na}_{2/3}\text{Ni}_{1/3}\text{Mn}_{2/3}\text{O}_2$. The $\text{Na}_{2/3}\text{Ni}_{1/3}\text{Mn}_{1/2}\text{Ti}_{1/6}\text{O}_2$ and $\text{Na}_{2/3}\text{Ni}_{1/3}\text{Mn}_{1/3}\text{Ti}_{1/3}\text{O}_2$ demonstrate higher capacity of $> 100 \text{mAh g}^{-1}$ with good retention. Moderate amount of titanium substitution for manganese in $\text{Na}_{2/3}\text{Ni}_{1/3}\text{Mn}_{2/3}\text{O}_2$ is found to be efficient to improve reversibility. Further structural investigation is under progress to study the improvement mechanism by titanium substitution.

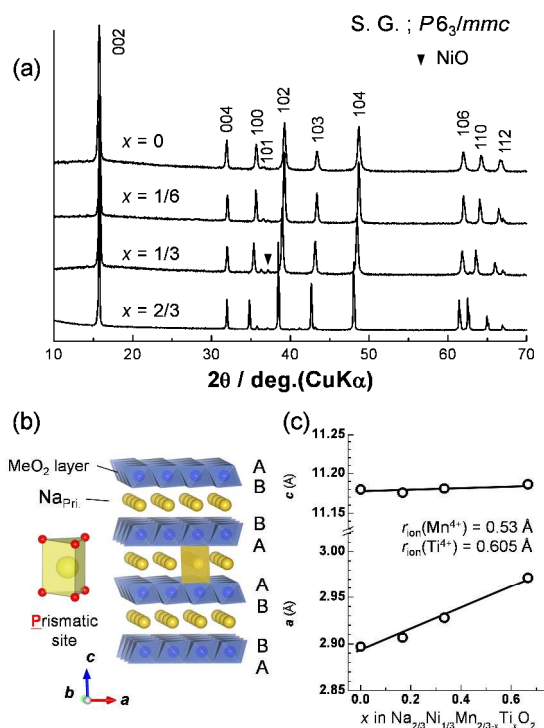


Figure 1. (a) XRD patterns of P2-type $\text{Na}_{2/3}\text{Ni}_{1/3}\text{Mn}_{2/3-x}\text{Ti}_x\text{O}_2$ ($0 \leq x \leq 2/3$) samples. (b) A schematic illustration of the crystal structure for P2-type $\text{Na}_{2/3}\text{Ni}_{1/3}\text{Mn}_{2/3-x}\text{Ti}_x\text{O}_2$ ($0 \leq x \leq 2/3$) drawn using the program VESTA¹⁴. (c) Changes in lattice parameters of $\text{Na}_{2/3}\text{Ni}_{1/3}\text{Mn}_{2/3-x}\text{Ti}_x\text{O}_2$ ($0 \leq x \leq 2/3$) samples.

When we compare the electrode performance and volume changes by Na extraction (see Table S1), it is concluded that Ti substitution is beneficial to suppress the volume change on charge/discharge, leading to the good cyclability.

Rate capability of the $\text{Na}/\text{Na}_{2/3}\text{Ni}_{1/3}\text{Mn}_{1/2}\text{Ti}_{1/6}\text{O}_2$ cell at rate of C/20 (12.1mA g^{-1}) - 2C (484mA g^{-1}) is examined in Fig. 3b. The C-rate is defined based on theoretical capacity calculated from $\text{Ni}^{2+/4+}$ redox for $\text{Na}_{1.0}\text{Ni}_{1/3}\text{Mn}_{2/3}\text{O}_2$, which equals to 241mAh g^{-1} . The cell delivers 80% of discharge capacity at 1C rate (241mA g^{-1}).

The capacity retention is further enhanced with a constant current and constant voltage (CC-CV) mode in Fig. 3c. In this test, the constant current (CC) charge/discharge mode was employed for initial 3 cycles, and then the CCCV mode (1 h for constant voltage) was employed from the 4th cycle. By using the CC-CV mode, the reversible capacity of about 120mAh g^{-1} is steadily obtained. It is thought that the capacity loss in the CC mode originates from the increase in electrode resistance associated with the high voltage operation. Therefore, studies on electrolyte additive¹⁵ and coating treatment¹⁶ could be effective to further improve the performance.

Figure 3d summarizes the reversible capacity and average potential experimentally obtained and estimated energy density of Na-ion full cells imaginarily consisting of different positive electrode materials and the hard-carbon negative electrode. In this study, we have found that $\text{Na}_{2/3}\text{Ni}_{1/3}\text{Mn}_{1/2}\text{Ti}_{1/6}\text{O}_2$ exhibits over 125mAh g^{-1} of reversible capacity with relatively high operating voltage of 3.7 V vs. Na^+/Na (on average). When we assume that hard-carbon delivers 300mAh g^{-1} with $E_{\text{ave.}} = 0.3 \text{V}$ vs. Na^+ , the energy density of hard-carbon/ $\text{Na}_{2/3}\text{Ni}_{1/3}\text{Mn}_{1/2}\text{Ti}_{1/6}\text{O}_2$ Na-ion cell is calculated to be 300Wh kg^{-1} based upon the total weight of positive/negative electrodes. This energy density is comparable to 290Wh kg^{-1} for a Li-ion cell of graphite (330mAh g^{-1} , $E_{\text{ave.}} = 0.2 \text{V}$)/ LiMn_2O_4 (100mAh g^{-1} , $E_{\text{ave.}} = 4.0 \text{V}$), and it attains 80% energy density of a graphite/ LiCoO_2 (150mAh g^{-1} , $V_{\text{ave.}} = 3.9 \text{V}$) cell (385Wh kg^{-1}). According to our knowledge and from Fig. 3d, $\text{Na}_{2/3}\text{Ni}_{1/3}\text{Mn}_{1/2}\text{Ti}_{1/6}\text{O}_2$ is one of the higher energy density materials for Na-ion battery among layered oxides reported so far.

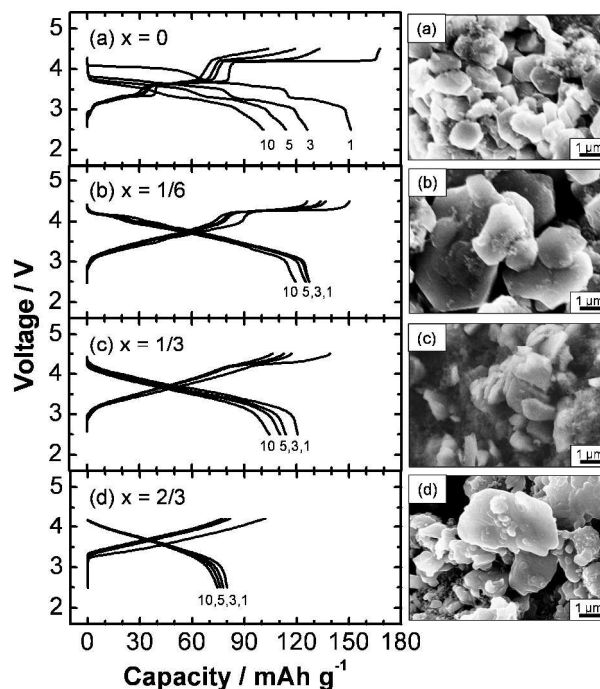


Figure 2. Charge/discharge curves of $\text{Na}_{2/3}\text{Ni}_{1/3}\text{Mn}_{2/3-x}\text{Ti}_x\text{O}_2$ ($0 \leq x \leq 2/3$) in Na cells at a rate of 12.1mA g^{-1} . Electrode morphology observed by SEM is also shown; $x =$ (a) 0, (b) 1/6, (c) 1/3, and (d) 2/3.

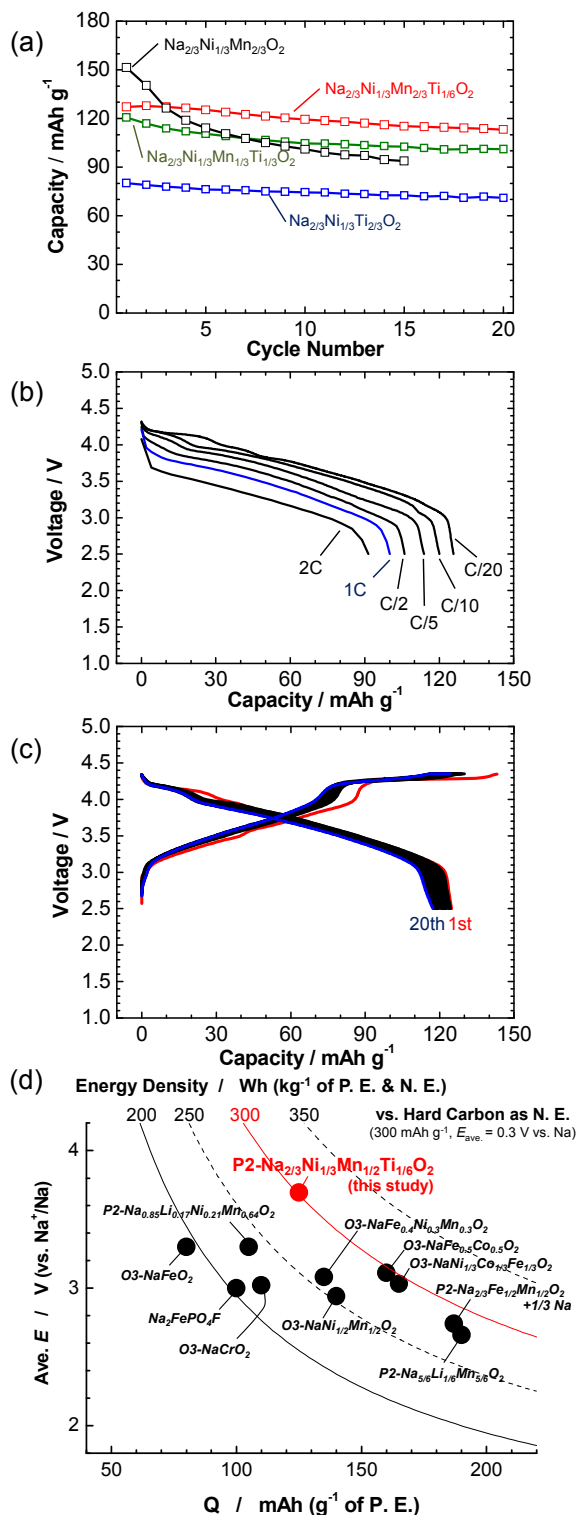


Figure 3. (a) Capacity retention of Na/Na_{2/3}Ni_{1/3}Mn_{2/3-x}Ti_xO₂ (0 ≤ x ≤ 2/3) cells. (b) Rate-capability of Na_{2/3}Ni_{1/3}Mn_{1/2}Ti_{1/6}O₂ in the Na cell. The cell was charged to 4.5 V at a rate of 12.1 mA g⁻¹ and then discharged at different rates; 1/20 (12.1 mA g⁻¹) – 2 C (480 mA g⁻¹). The sample loading on Al foil was 4.1 mg cm⁻² as the active material. (c) Charge/discharge curves with a CC-CV mode for the Na/Na_{2/3}Ni_{1/3}Mn_{1/2}Ti_{1/6}O₂ cell during 20 cycles (2.5–4.35 V). (d) Comparison of reversible capacity and average discharge voltage (vs. Na) experimentally obtained for the layered sodium insertion materials^{2-4, 6-8, 18-23}. The estimated energy density as full Na-ion cells is also shown with the hard-carbon as N.E. Herein, P.E. and N.E. stand for positive and negative electrodes, respectively. See the text for more details.

We believe, therefore, that Na-ion battery based on Na_xMeO₂ electrode has great possibility for the application to large format energy storage devices in future.

Conclusions

P2-type Na_{2/3}Ni_{1/3}Mn_{2/3-x}Ti_xO₂ (0 ≤ x ≤ 2/3) samples are prepared by heat treatment in air, and their electrode performance is compared in aprotic Na cells. The Na/Na_{2/3}Ni_{1/3}Ti_{1/6}Mn_{1/2}O₂ cell delivers 127 mAh g⁻¹ of reversible capacity with ca. 3.7 V of average discharge voltage versus Na⁺/Na. Estimated energy density as the positive electrode materials reaches 470 Wh kg⁻¹ based on the metallic sodium. We conclude that titanium substitution is the effective method to improve electrode performance of P2-type Na_{2/3}Ni_{1/3}Mn_{2/3}O₂.

Acknowledgements

This study was in part granted by JSPS through the “Funding for NEXT Program,” and MEXT program “Elements Strategy Initiative to Form Core Research Center” (since 2012), MEXT; Ministry of Education Culture, Sports, Science and Technology, Japan.

Notes and references

- S. P. Ong, V. L. Chevrier, G. Hautier, A. Jain, C. Moore, S. Kim, X. H. Ma and G. Ceder, *Energ Environ Sci*, 2011, **4**, 3680-3688.
- N. Yabuuchi, M. Kajiyama, J. Iwatate, H. Nishikawa, S. Hitomi, R. Okuyama, R. Usui, Y. Yamada and S. Komaba, *Nat Mater*, 2012, **11**, 512-517.
- N. Yabuuchi, M. Yano, H. Yoshida, S. Kuze and S. Komaba, *J Electrochem Soc*, 2013, **160**, A3131-A3137.
- H. Yoshida, N. Yabuuchi and S. Komaba, *Electrochem Commun*, 2013, **34**, 60-63.
- C. Delmas, J. J. Braconnier, C. Fouassier and P. Hagenmuller, *Solid State Ionics*, 1981, **3-4**, 165-169.
- S. Komaba, C. Takei, T. Nakayama, A. Ogata and N. Yabuuchi, *Electrochemistry Communications*, 2010, **12**, 355-358.
- N. Yabuuchi, H. Yoshida and S. Komaba, *Electrochemistry*, 2012, **80**, 716-719.
- J. Zhao, L. W. Zhao, N. Dimov, S. Okada and T. Nishida, *J Electrochem Soc*, 2013, **160**, A3077-A3081.
- S. Okada, Y. Takahashi, T. Kiyabu, T. Doi, J. Yamaki and T. Nishida, *ECSC Meeting Abstracts*, 2006, **602**, 201.
- Haijun Yu, Shaohua Guo, Yanbei Zhu, M. Ishida and H. Zhou, *Chem. Commun.*, 2014, **Advance Article**.
- C. Delmas, C. Fouassier and P. Hagenmuller, *Physica B & C*, 1980, **99**, 81-85.
- L. Zhonghua and J. R. Dahn, *J Electrochem Soc*, 2001, **148**, A1225-A1229.
- D. H. Lee, J. Xu and Y. S. Meng, *Phys. Chem. Chem. Phys.*, 2013, **15**, 3304-3312.
- K. Momma and F. Izumi, *J. Appl. Crystallogr.*, 2008, **41**, 653-658.
- S. Komaba, T. Ishikawa, N. Yabuuchi, W. Murata, A. Ito and Y. Ohsawa, *Acs Appl Mater Inter*, 2011, **3**, 4165-4168.
- S.-T. Myung, K. Izumi, S. Komaba, Y.-K. Sun, H. Yashiro and N. Kumagai, *Chem. Mater.*, 2005, **17**, 3695.
- S. Shimazu, T. Ishikawa, N. Yabuuchi, S. Shiraiishi, K. Gotoh, K. Takeda and S. Komaba, *The 53rd Battery Symposium in Japan, Abs. 2E22, Fukuoka, Japan*, 2012.
- S. Komaba, N. Yabuuchi, T. Nakayama, A. Ogata, T. Ishikawa and I. Nakai, *Inorg Chem*, 2012, **51**, 6211-6220.
- Y. Kawabe, N. Yabuuchi, M. Kajiyama, N. Fukuhara, T. Inamasu, R. Okuyama, I. Nakai and S. Komaba, *Electrochem Commun*, 2011, **13**, 1225-1228.
- Donghan Kim, Sun-Ho Kang, Michael Slater, Shawn Rood, John T. Vaughey, Naba Karan, Mahalingam Balasubramanian and C. S. Johnson, *Adv. Energy Mater.*, 2011, **1**, 333-336.
- R. Hara, N. Yabuuchi, M. Kajiyama, Y. Aoki and S. Komaba, *The 53rd Battery Symposium in Japan, Abs. 1B22, Fukuoka, Japan, Nov. 2012*.
- N. Yabuuchi, R. Hara, M. Kajiyama, K. Kubota, T. Ishigaki, A. Hoshikawa and S. Komaba, *submitted*.
- P. Vassilaras, A. J. Toumar and G. Ceder, *Electrochem Commun*, 2014, **38**, 79-81.